Liquid Crystals
Publication details, including instructions for authors and subscription information:
http://www.informaworld.com/smpp/title~content=t713926090

X-ray investigations on a homologous series of mesogenic azo compounds complexed with palladium (II)

A. M. Levelut[a]; M. Veber[ab]; O. Francescangeli[c]; S. Melone[c]; M. Ghedini[d]; F. Neve[de]; F. P. Nicoletta[ef]; R. Bartolino[ef]

[a] Laboratoire de Physique des Solides, Bt. 510, Université Paris-Sud, Orsay, France [b] Chimie et Electrochimie des Matériaux Moléculaires, Paris Cedex 05, France [c] Dipartimento di Scienza dei Materiali e della Terra, Università di Ancona, Ancona, Italy [d] Dipartimento di Chimica, Università della Calabria, Rende, Cosenza, Italy [e] INFM Unità di Cosenza, [f] Dipartimento di Fisica, Università della Calabria, Rende, Cosenza, Italy

To cite this Article Levelut, A. M. , Veber, M. , Francescangeli, O. , Melone, S. , Ghedini, M. , Neve, F. , Nicoletta, F. P. and Bartolino, R.(1995) 'X-ray investigations on a homologous series of mesogenic azo compounds complexed with palladium (II)', Liquid Crystals, 19: 2, 241 — 249
To link to this Article: DOI: 10.1080/02678299508031975
URL: http://dx.doi.org/10.1080/02678299508031975

LIQUID CRYSTALS, 1995, VOL. 19, NO. 2, 241–249

X-ray investigations on a homologous series of mesogenic azo compounds complexed with palladium (II)†

by A. M. LEVELUT*‡, M. VEBER‡§, O. FRANCESCANGELI¶, S. MELONE¶, M. GHEDINI†‖, F. NEVE‖††, F. P. NICOLETTA‡‡†† and R. BARTOLINO‡‡††

‡ Laboratoire de Physique des Solides, Bât. 510, Université Paris-Sud, 91405 Orsay, France

¶ Dipartimento di Scienza dei Materiali e della Terra, Università di Ancona, INFM Unità di Ancona, Via Brecce Bianche, I-60 131, Ancona, Italy

‖ Dipartimento di Chimica, Università della Calabria, 87036 Rende, Cosenza, Italy

‡‡ Dipartimento di Fisica, Università della Calabria, 87036 Rende, Cosenza, Italy

†† INFM Unità di Cosenza

§ Chimie et Electrochimie des Matériaux Moléculaires, UA429, ESPCI 10, rue Vauquelin, 75231, Paris Cedex 05, France

(*Received 9 December 1994; accepted 14 February 1995*)

The X-ray diffraction experimental data concerning a homologous series of *p*-alkyl-*p'*-alkoxy-azobenzene cyclopalladated chloro-bridged dimers, both as powder and monodomain samples, are reported. These results, compared with those obtained for the parent non-metallated materials, suggest a model for the molecular arrangement wherein the alkoxy and alkyl chains are roughly coplanar with the palladium-containing rigid core and, depending on the chain length, bent towards each other.

1. Introduction

Interest in new materials has been recently focused on metal containing liquid crystals [1]. Within this field, thermotropic orthopalladated complexes are currently studied [2–4].

Information concerning the nature and the features of mesogenic materials can be conveniently obtained by considering homologous series of compounds. Accordingly, to investigate the mesomorphic behaviour of bimetallic cyclopalladated mesogens, we have considered the compounds whose general formula is depicted in figure 1.

The complexes usually are isomeric mixtures (*c.* 1 : 1) of forms **A** and **B** [2 (c)]. We will hereafter refer to them as the two series **N** and **N'**, where $\mathbf{N} = (n + m)$ and we keep $n = 1$ ($m = 1, 2, 7, 12, 18$; therefore $2 \leq \mathbf{N} \leq 19$), and $\mathbf{N'} = (n + m)$ and we keep $m = 12$ ($n = 1, 2, 3$; therefore $13 \leq \mathbf{N'} \leq 15$). Of course $\mathbf{N} = 13$ will be equal to $\mathbf{N'} = 13$.

An account of the mesomorphic behaviour and macroscopic properties of compounds **2**, **3**, **8**, **13** and **14'** [5], as well as preliminary neutron and X-ray small angle scattering results concerning compound **13** [6] have been previously given. The results of the complete X-ray diffraction study performed on both series of complexed and free azobenzenes are now reported in § 3 and discussed in § 4.

The mesomorphism exhibited by these palladium mesogens shows that the incorporation of the Pd_2Cl_2 core between two organic mesogenic ligands causes (i) an increase in the transition temperatures, (ii) the occurrence of more ordered mesophases and (iii) a reversible macroscopic biaxiality.

Similar results were obtained also for bis[*N*-(4-

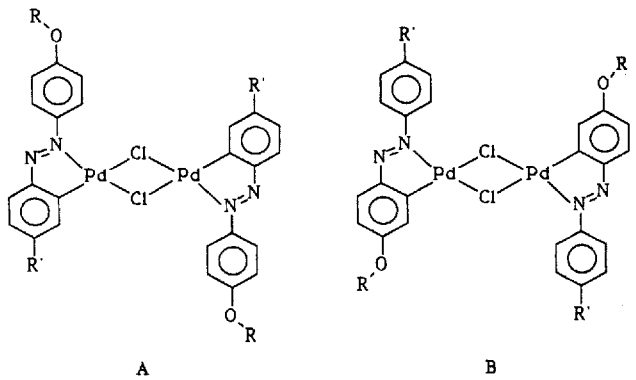

Figure 1. A sketch of the general structural formulae of the binuclear palladium complexes, where $R = C_m H_{2m+1}$, $R' = C_n H_{2n+1}$.

* Author for correspondence.

† Work partially supported by INFM under the cover of 'National Project on New Materials'.

0267–8292/95 $10·00

alkoxysalicylidene)-4′-alkylaniline] copper (II) complexes [7], a mesogenic series wherein the packing mode may be visualized as the result of an interdigitated molecular arrangement [8].

In principle, a similar interdigitated model could also be proposed for the palladium compounds. However, some differences concerning the molecular geometry have to be considered. The copper species are mononuclear complexes wherein a metal atom bridges two ligand molecules. In the present binuclear species, the bridge consists of the Pd_2Cl_2 fragment and, consequently, the palladium compounds become intrinsically biaxial and have a ligand-to-ligand distance larger than that for the copper compounds. Because of such a large distance, a simple interdigitated copper-like molecular array would give rise to empty inter- and intra-molecular spaces, which is not reasonable. Accordingly, the model has to be properly improved.

In the molecules of the compounds which form the **N** and **N′** series, three different parts can be roughly identified: (*a*) a rigid and nearly planar core (i.e. the two palladium-bonded aromatic rings and the Pd_2Cl_2 group); (*b*) a region with low mobility (i.e. the two remaining aromatic rings); (*c*) tails with both high mobility and flexibility (i.e. the four aliphatic chains).

Quasi elastic neutron scattering experiments carried out on compound **13** proved that the long alkoxy chains actually exibit a high mobility [9]. The above consideration suggests that a more appropriate packing model leading to the required space filling is obtained from molecules having the aliphatic chains folded and/or fused.

In this paper we report the X-ray investigations carried out on the **N** and **N′** complexes, and on the corresponding uncomplexed ligands (**LN** and **LN′**). The present study has been performed in order to elucidate the molecular arrangement exhibited by the dimeric chlorobridged mesogens and the role played by the metallic core in determining the mesomorphic behaviour of the compounds.

2. Experimental

The synthesis of the compounds was carried out as previously reported [2(c)]. The thermal behaviour was monitored by means of a Mettler FP 800 thermosystem equipped with an FP 84 microscopy cell, at a heating rate of $4°C\,min^{-1}$. The textures of the various mesophases were observed by means of a Zeiss Axioscope polarizing microscope equipped for photography and with a Linkam CO 600 heating stage.

X-ray diffraction measurements on powders were carried out with a conventional powder diffractometer allowing sufficiently high counting times. Ni filtered CuK_α radiation ($\gamma = 1{\cdot}54$ Å), strongly collimated with a system of slits, was used. The samples, with a thickness of 1·5 mm, were held by two thin Al sheets fixed to a circular hole in an Al matrix with a diameter of 1 cm. Heating was achieved by a hot stage with $\pm 0{\cdot}5°C$ accuracy and $\pm 0{\cdot}1°C$ stability.

X-ray measurements on monodomains were performed with a monochromatic beam issuing from a double bent graphite monochromator. The sample, held in a Lindemann glass capillary of 1 mm, was aligned by a 1·7 T magnetic field perpendicular to the X-ray beam and to the tube axis. The diffracted pattern was recorded on a cylindrical photographic film whose axis was parallel to the magnetic field. The maximum diffraction angle was limited to 22° in the direction of the magnetic field and to 60° perpendicular to it.

3. Results

The X-ray diffraction measurements were performed both on powder and monodomain samples and, for comparative purposes, both the uncomplexed azobenzenes (**LN** and **LN′**) and their palladated derivatives (**N** and **N′**) were examined. Moreover, X-ray investigations on monodomains have been carried out for the complexes **13** and **19**, and for the ligand **L13**. The different phases and the transition temperatures for the whole series and for the corresponding series of non-metallated azobenzenes are reported in table 1. Several of these compounds were previously investigated by optical and calorimetric techniques [5] and with reference to these data, in some cases differences concerning the transition temperatures or the mesomorphism were observed.

Regarding the ligands, as an example of the behaviour of the whole series, the powder spectra of **L13** recorded at different temperatures are given in figure 2.

The execution of a complete thermal cycle starting with a pristine sample shows that the low temperature solid Cr_1 present in the virgin sample is always different from the solid phase Cr_2 which forms on cooling from the melt, and can never be recovered. The different nature of these solid phases depends on the length of the aliphatic chains. Moreover, a comparison between the main periodicity of the structure, deduced from the smallest angle peak in the experimental patterns, and the lengths of the repeating molecular units in the fully extended conformations allows us to comment on the monolayered or bilayered nature of these solid phases. Therefore, for all the compounds except **L15′** and **L19**, Cr_1 is found to be crystalline and bilayered while Cr_2 is amorphous (or with a lower degree of crystallinity than Cr_1) and monolayered. We cannot decide about the layered nature of the Cr_1 phase of **L15′** and also of the Cr_1 and Cr_2 crystalline phases of **L19**, since the largest observed lattice spacing is 5·6, 4·6, and 4·2 Å, respectively. Obviously, the absence of lower angle diffraction rings is induced either by a textural effect

Table 1. The phase transitions of both the ligands and the complexes.

		Ligands†			Complexes†
L2		$Cr_1 \xrightarrow{90} Cr_2 \xrightarrow{105} I$; $Cr_2 \swarrow^{97}$	**2**‡		$Cr_1 \xrightarrow{190} Cr_2 \xrightarrow{236} N \xrightarrow{250} I$
L3		$Cr_1 \xrightarrow{96} Cr_2 \xrightarrow{126} I$; $Cr_2 \swarrow^{116}$	**3**‡		$Cr_1 \xrightarrow{120} Cr_2 \xrightarrow{235} N \xrightarrow{254} I$; $Cr_2 \xleftarrow[190]{} S_A \swarrow^{200}$
L8		$Cr_1 \xrightarrow{74} I$; $Cr_2 \xleftarrow[61]{} N \swarrow^{63}$	**8**		$Cr_1 \xrightarrow{76} Cr_2 \xrightarrow{190} N \xrightarrow{200} I$; $Cr_2 \xleftarrow{98} S_A \xleftarrow{140} N \swarrow^{175}$
L13	**L13′**	$Cr_1 \xrightarrow{66} Cr_2 \xrightarrow{76\cdot5} I$; $Cr_2 \xleftarrow[74]{} N \swarrow^{76}$	**13**	**13′**	$Cr_1 \xrightarrow{115} Cr_2 \xrightarrow{163} N \xleftrightarrow{179} I$; $Cr_2 \xleftarrow[100]{} S_A \swarrow^{145}$
	L14′	$Cr_1 \xrightarrow{55} Cr_2 \xrightarrow{72} I$; $Cr_2 \xleftarrow[65]{} S_A \xleftarrow[68]{} N \swarrow^{71}$		**14′**	$Cr_1 \xrightarrow{145} Cr_2 \xrightarrow{188} N \xleftrightarrow{195} I$; $Cr_2 \xleftarrow[175]{} S_A \swarrow^{179}$
	L15′	$Cr_1 \xrightarrow{70} S_A \xrightarrow{77} N \xrightarrow{81} I$; $Cr_2 \xleftarrow[57]{} S_A \xleftarrow[74]{} N \swarrow^{78}$		**15′**	$Cr \underset{130}{\overset{150}{\rightleftharpoons}} S_A \underset{160}{\overset{166}{\rightleftharpoons}} N \underset{166}{\overset{174}{\rightleftharpoons}} I$
L19		$Cr_1 \xrightarrow{86} I$; $Cr_2 \swarrow^{69}$	**19**		$Cr_1 \xrightarrow{115} Cr_2 \xleftrightarrow{130} S_A \xleftrightarrow{136} N \xleftrightarrow{160} I$

† Cr = solid; S = smectic; N = nematic; I = isotropic.
‡ For temperatures above *c.* 230°C some decomposition is observed.

or by an anisotropic disordering of the material. The mesomorphic ligands **L8**, **L13′**, **L14′** and **L15′** exhibit nematic and/or smectic mesophases (see the table) and their diffraction patterns are as expected for rod-like thermotropic compounds, i.e. a diffuse peak (in the nematic phase) or a sharp narrow peak (in the smectic phase) in the low angle region, together with a broad halo in the high angle region corresponding to about 4·5 Å (i.e. roughly the aromatic ring width). Furthermore, the lamellar thickness in the smectic phase of **L14′** and of **L15′** is fairly high compared to the molecular length. Similarly, as shown in figure 3, the largest period in the mesophase is also above the molecular length for the ligand **L13′**.

As an example of the experimental results concerning cyclopalladated samples, the X-ray diffraction spectra referring to complexes **3** and **15′** are reported in figures 4 and 5, respectively.

As in the parent **LN** and **LN′** compounds, all the solid palladated derivatives except **15′** exhibit two different phases, Cr_1 and Cr_2, the former existing only in the virgin sample. The different diffraction patterns observed for the two solid phases suggest for Cr_2 a higher degree of crystallinity and a layer periodicity which is twice that of Cr_1. The layer thickness in the Cr_1 solid (as well as in the single solid phase exhibited by sample **15′**) is comparable to the length of the complex.

The diffraction pattern of the mesophases shows a diffuse peak at 4·5 Å, sharper than in the ligands, and a further peak, more diffuse, centred at about 9·8 Å.

The layer spacings deduced from the position of the first peak at low angle are reported in table 2 for the different

phases of both the ligands and the complexes. The layer thickness in the smectic A phase is larger than the layer thickness in the Cr_1 phase or than half the layer thickness in Cr_2.

The dependence of the main periodicity on temperature for **13′** and **19** is given in figures 6 and 7, respectively.

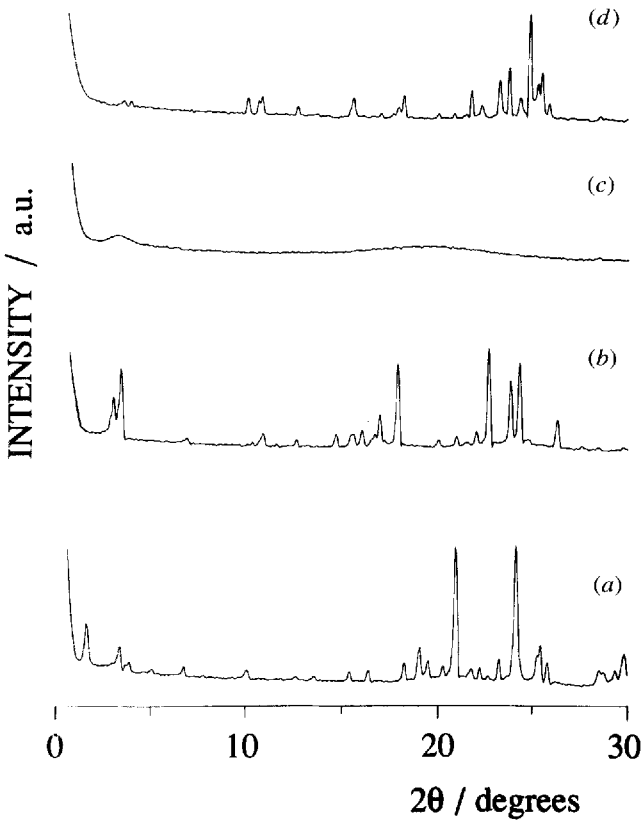

Figure 2. X-ray powder diffraction spectra for the free ligand **L13** obtained at different temperatures between room and isotropization temperatures in a heating–cooling thermal cycle. Heating cycle: (*a*) $T = 25°C$; (*b*) $T = 70°C$. Cooling cycle: (*c*) $T = 75°C$; (*d*) $T = 25°C$.

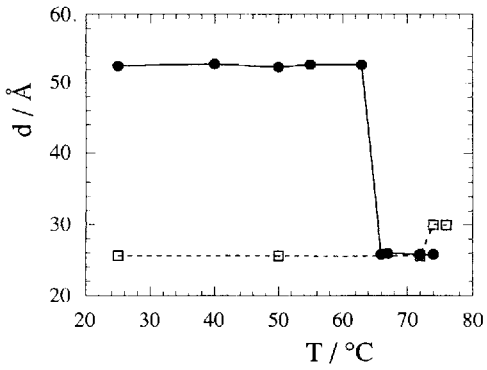

Figure 3. The behaviour of the main periodicity as a function of temperature for ligand **L13** = **L13′** (dots are for heating; squares are for cooling).

Finally, figure 8 shows a 2D diffraction pattern obtained from a monodomain; the diffraction pattern shown is for the quenched S_A phase of compound **13′**. Arrow (*a*) indicates a diffuse arc located in the equatorial plane, corresponding to intra-layer interferences between organic moieties ($2\vartheta \cong 20°$ with $\lambda = 1{\cdot}54$ Å). Arrow (*b*) indicates a second inner diffuse arc at $2\vartheta \cong 9°$ and also located in the equatorial plane, which characterizes the Pd_2Cl_2–Pd_2Cl_2 intra-layer interferences. Finally, arrow (*c*) shows the presence of a set of Bragg reflections which the layers form on both sides of the beam stop, along the meridian. The magnetic field H is parallel to the normal to the layers. The difference between the mesophases of these complexes and the same mesophase of organic ligand, effective for the whole series of compounds, is apparent from the scattered intensities observed for sample **13′** in the smectic A phase, both in the equatorial and meridianal direction; along the meridian, reflections by the layer structure are visible to the third order, attesting a good localization of the Pd_2Cl_2 groups, while the Pd_2Cl_2–Pd_2Cl_2 intra-layer interferences characterize a preferred distance of ~ 10 Å, which is characteristic of a side-by-side, locally biaxial intra-layer array of the

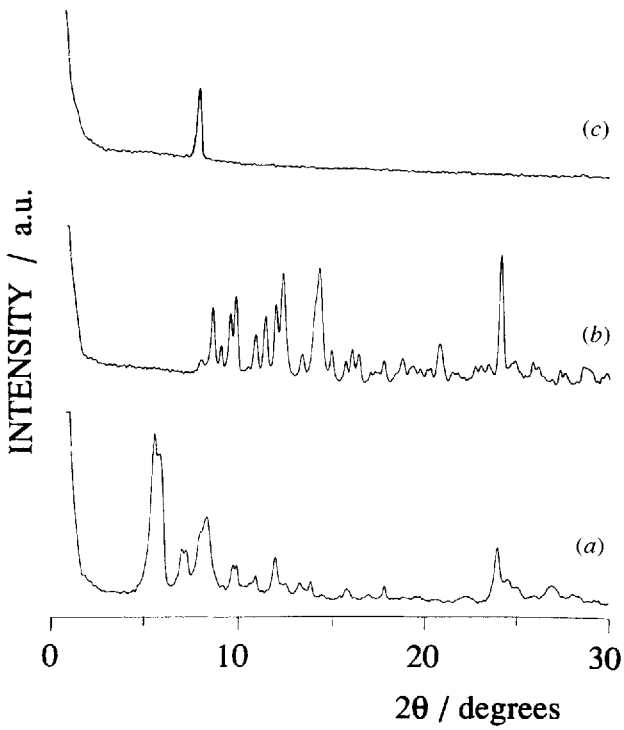

Figure 4 X-ray powder diffraction spectra for the palladium complex **3** obtained in a heating–cooling cycle at different temperatures between room and isotropization temperatures. Heating cycle: (*a*) $T = 25°C$; (*b*) $T = 150°C$. Cooling cycle: (*c*) $T = 195°C$.

complexes [8 (b)]. Conversely, the layer periodicities for the ligands are comparable to those estimated for the corresponding complexes.

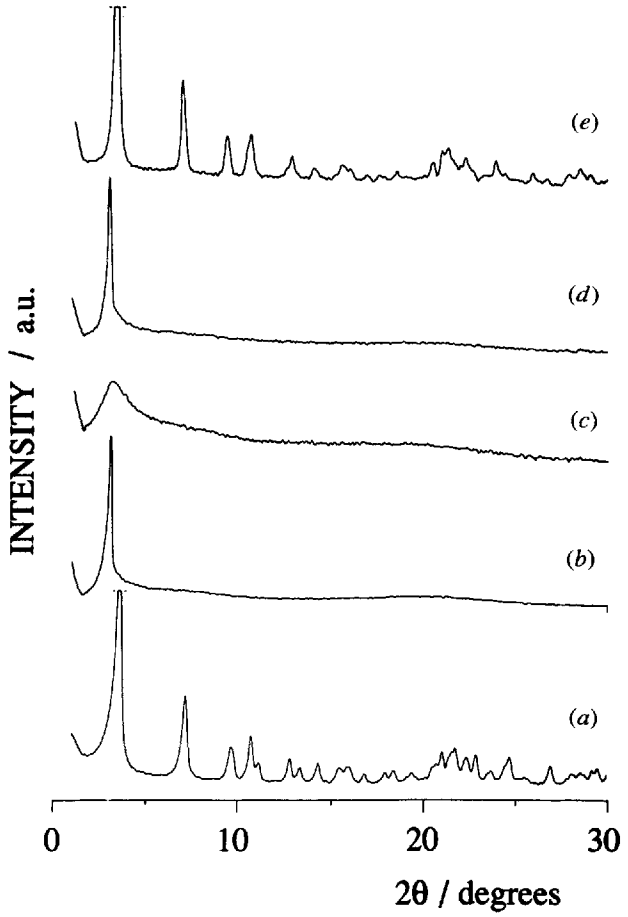

Figure 5. X-ray powder diffraction spectra for complex **14′** obtained at different temperatures between room and isotropization temperatures in a heating–cooling thermal cycle. Heating cycle: (*a*) $T = 25°C$; (*b*) $T = 155°C$; (*c*) $T = 170°C$. Cooling cycle: (*d*) $T = 150°C$; (*e*) $T = 25°C$.

Table 2. Layer spacings (Å) for the different phases of the ligands and of the complexes: Cr_1, virgin solid, Cr_2, second solid phase, M, smectic A and/or nematic phase. ‡ Cr_2 is actually identical to Cr_1,† see text.

	Ligands			Complexes		
N/N′	Cr_1	Cr_2	M	Cr_1	Cr_2	M
2	16·0	8	—	13·5	20·2	10·1
3	20·0	10·9	—	16·1	21·0	10·3
8	40·0	20·0	20·0	16·2	35·0	17·9
13/13′	52·0	25·8	30·0	22·5	45·5	30·0
14′	50·2	25·2	29·9	24·1	48·0	29·9
15′	†	28·6	30·7	25·1	‡	29·2
19	†	†	—	27·5	57·2	38·9

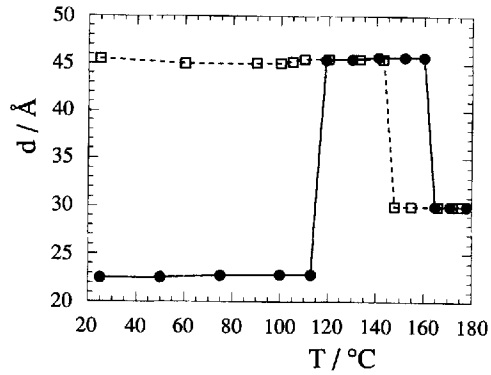

Figure 6. The behaviour of the main periodicity as a function of temperature for complex **13′** (dots are for heating; squares are for cooling).

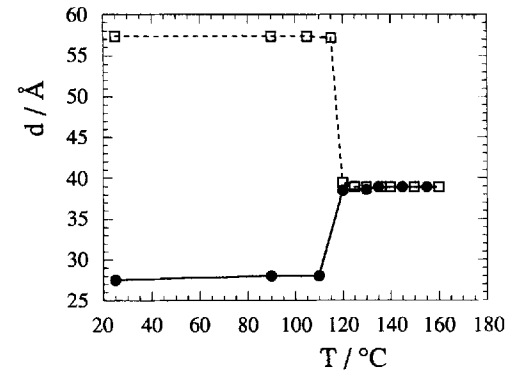

Figure 7. The behaviour of the main periodicity as a function of temperature for complex **19** (dots are for heating; squares are for cooling).

4. Discussion

A first point that we must consider is the enhancement of the mesogenic behaviour as evidenced by the mesomorphic properties, since the complexes with almost no chains (**N** = 2 and 3) present a mesophase. Another surprising point is the significant supercooling for all the complexes except those at the termini of the series (i.e. **2** and **19**). This supercooling is observed for transitions between two mesophases and less often at the clearing transition. This unexpected behaviour can be related to the fact that the complexes are in fact isomeric mixtures: disordered organizations are thus favoured, at least at high temperatures, by the presence of two isomers. (This explanation cannot however provide the whole story, since the isomeric *purity* of complex **8** [2 (c)] contradicts it.) Moreover, taking into account the high viscosity of the fluid phases, one can understand that transitions towards more and more ordered phases are not easy.

The X-ray data give access to the molecular organization of each phase. For the crystalline phases, it is clear that complete information could not be derived from our

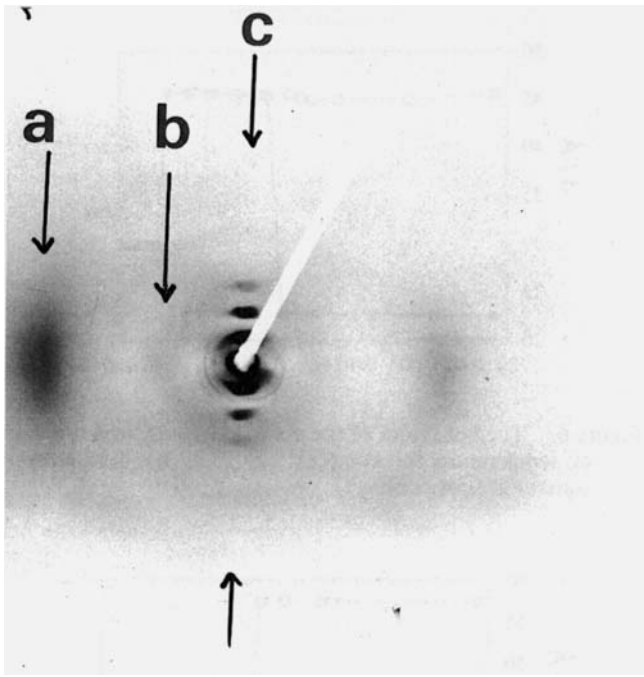

Figure 8. A 2D image of the diffraction pattern for a monodomain of the complex **13′**.

diffractograms since even the unit cell has not been determined. However, obviously all the crystalline phases here studied are lamellar, the thickness of the lamellae being characterized by the position of small angle Bragg peaks. Moreover, owing to the similarity of the crystalline polymorphism of the ligands and the corresponding complexes on the one hand, and on the other hand, of nearly all the homologues in a given series, it is possible to derive some semi-quantitative conclusions about the evolution of the molecular organization. Finally we notice that of the two crystalline phases of the same compound, one is bilayered while the second is monolayered.

In a smectic phase the molecular packing can be characterized by the layer thickness, the orientation of the director with respect to the layer normal and the mean area per molecule in the layer plane. In a smectic A phase, the director is perpendicular to the layer plane and in most cases, the layer periodicity is nearly equal to the actual molecular length. In the nematic phase, the position of the inner ring can also be compared to the molecular length, except if one approaches a transition to a smectic C of large tilt angle ($> 40°$).

Therefore the apparent molecular length, hereafter designated AML, will be the guideline in the following discussion. In the monolayered solid and in the smectic A phases, AML is equal to the layer periodicity, in the nematic phase, AML is related by the Bragg relation to the position of the inner ring, and in the bilayered crystalline phase, AML is taken as equal to one half of the layer thickness.

4.1. *The ligands*

In a homologous series of calamitic liquid crystals, owing to their elongated molecular shape, the AML should be an increasing function of the number of carbon atoms which form the aliphatic chains. Now, in a crude molecular model wherein the aliphatic chains are extended in prolongation of the elongated core and in an all-*trans*-conformation, each added CH_2 group will increase the AML value by about 1·25 Å. However, it has to be taken into account that such an increment depends on the state of organization of the phase being considered, being close to 1·25 Å in the solid phase (wherein generally the chains are in an all-*trans*-conformation), whereas, in the mesophase, the increment of AML per added methylene is subject to conflicting effects. The global thermal motion of the molecules gives a trend to increased AML values, while the thermal *trans*-to-*cis*-conformational scrambling, which is more and more effective as the chain length increases, has the contrary effect.

The ligand molecules **LN** and **LN′** can be considered as rod-like molecules and therefore the AML dependence versus the total number of aliphatic carbon atoms will provide some information about the chain conformation in the different phases (see figure 9).

In the two solid phases, it is clear that the AML increases linearly with the total number of carbon atoms, independently of the specific chain (alkyl or alkoxy) under consideration. Moreover the plot shows a slope of about 1·45 Å per carbon for both the Cr_1 and Cr_2 solid phases, a slope which becomes 1·61 Å in the nematic phase. Consequently, the experimental AML values are in agreement with the data expected for molecules whose aliphatic chains adopt the all-*trans*-conformation, at least for the solid phase. However the slope of 1·61 Å/CH_2 for

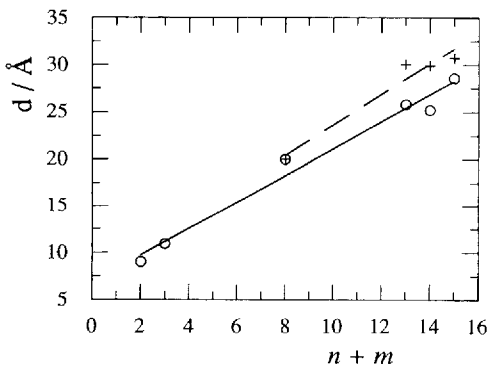

Figure 9. Behaviour of the apparent molecular length (AML), in Å, for the ligands against the total number of carbons in the aliphatic chains $(m + n)$. The lower curve fits the experimental points for the solid phases (circles) of the ligands (slope 1·45), whereas the upper curve fits the experimental points for the mesophases (crosses) (slope 1·61). The limiting values for $n + m = 0$ are about 7 Å for the solid and 7·5 Å for the mesophase.

AML in the mesophase of the ligand exceeds the value usually observed for smectogenic molecules. For example, this slope is nearly 1 Å for the S_A phase of the *N*-(4-alkoxysalicylidene)-4′-alkylanilines series [8(c)], which has a similar core. The high value of this slope corresponds to a rather large value of the AML compared to the theoretical length measured using models: AML is 29·5 Å for **N** = 13 compared to ≅ 27·5 Å for the homologous member of the above mentioned series. Simultaneously, the length of core which corresponds to AML (**N** = 0) is surprisingly small (7·5 Å compared to ≈ 11 Å measured from a model). The origin of this apparently strange behaviour could be explained both by the fact that the ligand presents only a nematic phase, and only for a very few members of the series. Accordingly the AML is not really significant in a nematic phase, and moreover the determination of the slope and of the core length is not accurate, since only a few members of the series have a nematic phase.

4.2. *The complexes*

The organometallic complexes **N** and **N′** are lateral-lateral fused mesogens [10] and display a slightly asymmetric H-like molecular shape with a rigid central core (sized about 11 × 12 Å^2) and four aliphatic chains. The identical chains (alkyl or alkoxy) are on the same diagonal of the H, so that the molecular length of the complex results from the length of the central core (about 11 Å) plus the sum of the two longer chains. Therefore, along the homologous series **N** and **N′**, the addition of a further CH_2 group in the ligand's aliphatic chains will increase the molecular length of the complex only if the addition occurs in the longer chain.

The AML values resulting from **N** and **N′**, are close to those found for the parent ligands **LN** and **LM′**, the alkyl chain remaining very short in all cases studied. Nevertheless, their plots against the number, *n* or *m*, of aliphatic carbons, respectively show interesting features.

In particular, with reference to compounds having *m* = 12 and *n* = 1, 2, 3 (**N′** series, (see figure 10)) the AML values for the mesophases follow the expected trend and are unaffected by *n*. Conversely in the solids Cr_1 and Cr_2, the AML progressively increases with *n*.

With reference to the series wherein *m* varies (**N** series, see figure 11), the AML values concerning either the Cr_1 or the Cr_2 solid phases increase with *m*. However, it should be pointed out that the increase is in both cases smaller than that theoretically calculated for fully elongated molecules (whose plot should have a slope of 1·25 × 2 Å per CH_2).

Furthermore, the influence exerted by *m* is lower in the monolayered solid Cr_1 (0·8 Å per CH_2) than in the bilayered solid Cr_2 (1·1 Å per CH_2). The measurements carried out on the mean increment in AML values of the mesophases is 1·78 Å per CH_2. This increment is higher

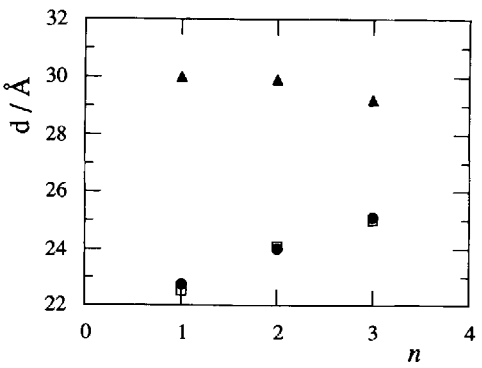

Figure 10. AML behaviour as a function of the number of carbons in the short chain (*n*) in the solids and in the smectic phases of the complexes (**N′** series): the open squares are for Cr_1 (virgin solid), the triangles for the mesophases and the full dots for Cr_2 (final solid).

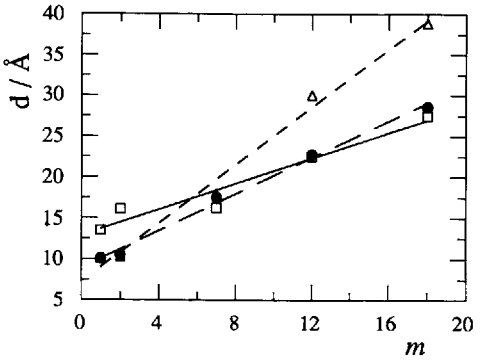

Figure 11. AML behaviour as a function of the number of carbons in the long chain (*m*) in the two solids and in the smectic phases of the complexes (**N** series): the open squares are for Cr_1 (virgin solid), the triangles for the mesophases and the full dots for Cr_2 (final solid).

than that found for the solid phases and comparable with that of the mesophases of the ligands (i.e. 1·61 Å per CH_2).

Remarkably, the AML values for the nematic phases are greater than for the solid phases only for the longest chains ($m \geq 7$), and equal or smaller for the shortest chains.

As we have already pointed out, the estimation of the AML value in a solid phase does not provide very reliable information about the molecular packing in this phase. The low values of the mean increment of the layer thickness per CH_2 has to be related to the compact packing of complexes of asymmetric H shape in the solid phases, with the longest diagonal of the H tilted with respect to the normal to the layer planes. However, comparison with the mesophase behaviour could help us to understand the molecular organization of the mesophase. In the mesophase the other important parameter to be considered is the mean area per chain, which is directly related to the mean molecular area.

In the mesophases of the complexes, a linear dependence of AML is observed with m, while AML does not depend on n. Therefore it seems that the alkyl chain is too short and does not increase the layer thickness of a S_A phase. That is, the complex can be considered as built of a large core including the alkyl chains, surrounded symmetrically by the two alkoxy chains. The total number of carbons is $2m$, and the apparent molecular length increases linearly with m: AML $= L_c + \alpha m$. The half slope $\alpha/2$ is 0·89 Å/CH_2 and gives the increment of AML for each new CH_2 group; this value can be easily compared to the usual values ($\cong$ 1 Å), while the extrapolated value for $m = 0$, 7·2 Å is obviously shorter than the core length, as for the ligand. These two lengths allow us to estimate the ratio between the core and the chain densities ρ_c and ρ_{ch}, respectively. If it is assumed that the linear dependence of AML versus m, AML $= L_c + \alpha m$ implies a constant molar area, this area will be that of the core and of any CH_2 group. Therefore the volume ratio between the core and a methylene group is

$$\frac{2L_c}{\alpha} \quad \text{and,} \quad \frac{\rho_{ch}}{\rho_c} = \frac{M_{CH_2}}{M_c}\frac{2L_c}{\alpha}$$

where, M_{CH_2} and M_c are the mass of a methylene group and of the core respectively.

In fact, in writing down this expression, we have to keep in mind not only that the core includes only the short alkyl chains, but also the difference in volume between methyl end groups and methylene groups. Under the assumption that molecular areas are independent of the chain length, the core has a sixfold higher density than the chains. This large ratio can be explained on the one hand by the fact that the core, which contains the heavy Pd_2CL_2 subunit, is confined (following our assumption in a thin layer—7·2 Å compared to the expected core length—11 Å) and on the other hand by the highly disordered state of the chains that are attached to a large core.

Assuming a chain density of 0·5 g cm^{-3}, the molecular area should be 47 Å^2, which holds as well for the core and the chains, and the mean density of the mesophase is 1·1 g cm^{-3} for compound **19** and 2·6 g cm^{-3} for compound **2**. This mean area is consistent with the core dimensions 11 × 10 × 4·5 Å. However the apparent core length is underestimated in this model. In fact the AML value of the two first homologues is consistent with a model in which the terminal groups of two adjacent layers are interdigitated; in other words the small apparent core length value is a measure of the overlap of the two ligands linked by the Pd_2Cl_2 subunit.

The fact that AML is independent of n and increases linearly with m can be related to the fact that the long chain (of length m) has a tendency to fill the free space close to the short chain. Considering this tendency to a best occupancy of the space, we have to examine the global AML dependence versus $m + n$. The previous discussion applies again, but we now consider that each paraffinic sublayer on each side of the core sublayer contains one alkyl and one alkoxy chain, in such a way that the core area is equal to twice the chain area. In order to take into account the asymmetric H geometry of the core, we also include the terminal methyl groups in the core, considering consequently that the first homologue **2** is at the origin of the series with a $m + n - 2$ chain length. Taking into account the slightly different values for the slope of AML versus $m + n$ (1·72 Å) and of the core length (10·2 Å), we can estimate the chain to core density ratio to be 0·23 and the core area to be 49 Å^2, under the assumption of a chain density of 0·55 g cm^{-3}, the mean density varying from 2·4 g cm^{-3} for $\mathbf{N} = 2$ to 1·04 g cm^{-3} for $\mathbf{N} = 19$. Obviously the two models are very similar, the only difference being the chain area, which is of 25 Å^2 in the second interpretation. However, in this model, the interface between two layers is shared by all the chains independently of their length. Therefore the mean chain area has a value which compares to usual smectogenic molecules [11]. This model gives a good description of the organization of the shortest homologues. As the chain length is increased, the difference between these complexes and the usual rod-like mesogen is obvious: the low value of the chain density means that a long chain cannot fill compactly the empty space around a short chain.

It appears that, contrary to the copper complexes (but with a single copper atom), interdigitation of the chains from adjacent layers is not allowed. The tendency of the long chain of a complex to fill the free space left by the short chain of the same complex ensures a global lath shape to the complex which must be considered in relation to a biaxial behaviour.

5. Conclusions

The discussions on the molecular geometry displayed by the **N** and **N′** complexes in relation to the packing properties, as deduced from arguments concerning the AML and area per chain, brings us to the conclusion that the interdigitated model fails. At the moment, we are unable to enter into the microscopic details of the origins of such a behaviour. But we can observe that the bimetallic bridge $(Pd–Cl)_2$ sterically leaves the two mesogenic ligand moieties at a larger distance than in mononuclear complexes (as for example the Cu complexes). Moreover, the electronic density arising from the two metals is so high that electric multipolar interactions cannot be excluded. However, on the basis of both steric and multipolar electrical interactions and according to Dowell's arguments [12] (with reference, in that case, to the re-entrant phenomena in polar liquid crystals), we suggest that the rigid cores have a high degree of order and a strong tendency to remain crystallized (so conferring

high transition temperatures on the mesogens). In addition, the only way to obtain a partial loss of the positional order seems to be by the increase in entropy through the disorder induced by the presence of flexible chains. Therefore, the filling of the molecular empty spaces in the complexes **N** and **N′** is achieved by a continuous dynamical curvature of the aliphatic chains (instead of by interdigitation of the molecules) or by an increase in the area occupied by the longest chains.

This work was financed by the Italian CNR and INFM under the auspices of 'Progetto Finalizzato Materiali Speciali per Tecnologie Avanzate' and the 'National Project on New Materials', respectively. We thank Johnson Matthey Ltd for a generous loan of $PdCl_2$.

References

[1] (a) GIROUD-GODQUIN, A. M., and MAITLIS, P. M, 1991, *Angew. Chem., Int. Ed. Engl.*, **30,** 375; (b) ESPINET, P., ESTERUELAS, M. A., ORO, L. A., SERRANO, J. L., and SOLA, E., 1992, *Coord. Chem. Rev.*, **117,** 215; (c) BRUCE, D. W., and O'HARE, D., editors, 1992, *Inorganic Materials* (Wiley); (d) HUDSON, S. A., and MAITLIS, P. M., 1993, *Chem. Rev.*, **93,** 861; (e) POLISHCHUCH, A. P., and TIMOFEEVA, T. V., 1993, *Russ. Chem. Rev.*, **62,** 291.

[2] (a) GHEDINI, M., LONGERI, M., BARTOLINO, R., 1982, *Molec. Crystals liq. Crystals*, **84,** 207; (b) GHEDINI, M., LICOCCIA, S., ARMENTANO, S., and BARTOLINO, R., 1984, *Molec. Crystals liq. Crystals*, **108,** 269; (c) GHEDINI, M., ARMENTANO, S., and NEVE, F., 1987, *Inorg. Chim. Acta*, **134,** 23; (d) GHEDINI, M., PUCCI, D., DE MUNNO, G., VITERBO, D., NEVE, F., and ARMENTANO, S., 1991, *Chem. Mater.*, **3,** 65.

[3] (a) BARBERA, J., ESPINET, P., LALINDE, E., MARCOS, M., and SERRANO, J. L., 1987, *Liq. Crystals*, **2,** 833; (b) MARCOS, M., ROS, M. B., and SERRANO, J. L., 1988, *Liq. Crystals*, **3,** 1129; (c) ESPINET, P., ETXEBARRIA, J., MARCOS, M., PEREZ, J., RAMON, A., and SERRANO, J. L., 1989, *Angew. Chem., Int. Ed. Engl.*, **28,** 1065; (d) ESPINET, P., LALINDE, E., MARCOS, M., PEREZ, J., and SERRANO, J. L., 1990, *Organometallics*, **9,** 555.

[4] HOSHINO, M., HASEGAWA, H., and MATSUNAGA, Y., 1991, *Liq. Crystals*, **9,** 267.

[5] VERSACE, C. C., BARTOLINO, R., GHEDINI, M., NEVE, F., ARMENTANO, S., KIROV, N., and PETROV, N., 1990, *Liq. Crystals*, **8,** 481.

[6] FORMOSO, V., PAGNOTTA, M. C., MARIANI, P., GHEDINI, M., NEVE, F., BARTOLINO, R., MORE, M., and PEPY, G., 1992, *Liq. Crystals*, **11,** 639.

[7] (a) GHEDINI, M., ARMENTANO, S., BARTOLINO, R., RUSTICHELLI, F., TORQUATI, G., KIROV, N., and PETROV, M., 1987, *Molec. Crystals liq. Crystals*, **151,** 75; (b) GHEDINI, M., ARMENTANO, S., BARTOLINO, R., KIROV, N., PETROV, M., and NENOVA, S., 1988, *J. molec. Liq.*, **38,** 207.

[8] (a) GHEDINI, M., ARMENTANO, S., BARTOLINO, R., TORQUATI, G., and RUSTICHELLI, F., 1987, *Sol. St. Commun.*, **64,** 1191; (b) LEVELUT, A. M., GHEDINI, M., BARTOLINO, R., NICOLETTA, F. P., and RUSTICHELLI, F., 1989, *J. Phys. (France)*, **50,** 113; (c) TORQUATI, G., FRANCESANGELI, O., GHEDINI, M., ARMENTANO, S., NICOLETTA, F. P., and BARTOLINO, R., 1990, *Il Nuovo Cimento*, D, **12,** 1363; (d) GHEDINI, M., MORRONE, S., GATTESCHI, D., and ZANCHINI, C., 1991, *Chem. Mater.*, **3,** 752.

[9] BARTOLINO, R., CODDENS, G., RUSTICHELLI, F., PAGNOTTA, M. C., VERSACE, C. C., GHEDINI, M., and NEVE, F., 1992, *Molec. Crystals liq. Crystals*, **221,** 101.

[10] LEVELUT, A. M., 1992, *Molec. Crystals liq. Crystals*, **215,** 31.

[11] GUILLON, D., and SKOULIOS, A., 1978, *J. de Physique*, **38,** 79.

[12] DOWELL, F., 1987, *Phys. Rev., A*, **36,** 5046.